Supporting Information for:

The pH-dependence of copper(II/I) reduction potentials in variants of *P. aeruginosa* azurin with surface histidine variations

Sara Ghodrati Dolatshamloo, Nikta Ghazi, Jeffrey J. Warren*

Department of Chemistry
Simon Fraser University
8888 University Drive
Burnaby BC V5A 1S6
Canada

*jjwarren@sfu.ca

Contents:

Material and Methods 2
Representative UV-visible spectrum of azurin 4
MALDI mass spec data for azurin variants 5
Example electrochemical data for azurins 8
Snapshots of histidine local environments in MD cluster structures 9
Comparison of per-residue fluctuations (RMSF) in MD simulations of azurin. 21
Comparison of azurin RMSD values over the course of MD simulations 22
Computationally predicted histidine pK_a values 24
Plots of pK values as a function of Cu-histidine distance 25
Plots of $E°´$ values as a function of Cu-histidine distance 26

Material and Methods

Expression and Purification of Azurin Variants. The wild-type Az plasmid in the pET3a vector was a gift from John H. Richards (California Institute of Technology). Plasmids encoding for each Az variant were prepared using an established polymerase chain reaction (PCR) technique for introduction of point mutations (see main text for citations). Introduction of mutations was confirmed by Sanger sequencing from Azenta Life Sciences. The forward and reverse PCR primers used for each point mutation are set out below. All sequences are listed 5´ to 3´.

H83Q forward: CGC CCA GAC CAA GCT GAT CGG ATC CGG TGA AAA AGA C

H83Q reverse: GCT TGG TCT GGG CGA TAA CTC GAG AGT CAT CCG G

Q107H forward: GGT GAA CAC TAC ATG TC TC TGC ACT TC C

Q107H reverse: CAT GTA GTG TC ACC TC TTT AAG CTT GGA AAC G

M109H forward: GAA CAG TAC CAC TC TC TGC ACT TC CCG GGT CAC

M109H reverse: GCA GAA GAA GTG GTA CTG TC ACC TC TTT AAG C

K122H forward: CTG ATG CAT GGT ACC CTG ACT CTG AAA TAG AGA TCC G

K122H reverse: GGT ACC ATG CAT CAG TGC GGA GTG ACC CGG GAA AG

T124H forward: GAA AGG TCA CCT GAC TCT GAA ATA GAG ATC CGG C

T124H reverse: GTC AGG TGA CCT TC ATC AGT GCG GAG TGA C

T126H-forward: CCC TGC ATC TGA AAT AGA GAT CCG GCT GC

T126H reverse: CTA TTT CAG ATG CAG GGT ACC CTT CAT CAG TGC GG

Each of the known Az variants were expressed and purified to homogeneity. Protein integrity was assessed via UV-Vis spectroscopy and MALDI-TOF mass spectrometry. Briefly, Azurin mutant plasmids were transformed into chemically competent BL21(DE3) *E. coli*, selected on LB agar with 100 μg/mL ampicillin (37°C, 16 hours). A single colony was grown in 25 mL LB with ampicillin (37°C, 180 rpm, 16 hours). A 10 mL starter culture was used to inoculate 1 L Terrific Broth (TB) medium with 0.4% glycerol and ampicillin, grown at 37°C, 180 rpm for 17.5 hours. Cells were harvested by centrifugation (7000 g, 15 min, 4°C).

For osmotic shock, pellets were resuspended in 50 mM Tris (pH 8.1) with 1 mM EDTA and 20% sucrose, incubated at 4°C for 20 min, and centrifuged (12,000 g, 20 min, 4°C). The pellet was then resuspended in 500 μM $MgCl_2$, incubated for 20 min at 4°C, and centrifuged again. Azurin metalation was achieved by adding 100 mM $CuSO_4$ and 500 mM sodium acetate (pH 4.5) dropwise. The light blue solution was incubated (37°C, 180 rpm, 21.5 hours) and centrifuged (12,000 g, 20 min, 4°C).

Purification was conducted on a CM Sepharose column equilibrated with 5 mM sodium acetate (pH 4), eluting azurin with a 0–100 mM sodium acetate gradient (pH 4.5). Fractions containing azurin were pooled and concentrated. UV–Vis spectra were recorded with a Cary 100 Bio spectrophotometer to check Azurin purity.

Protein Mass Analysis by MALDI-TOF mass spectrometry. MALDI-TOF was used to verify the molecular weight of wild-type and engineered azurin variants. Prior to analysis, proteins were buffer-exchanged into deionized water and mixed in a 1:1 ratio with a saturated sinapinic acid

(molecular weight 224.21 g/mol) matrix solution (prepared in 30:70 acetonitrile:0.1% trifluoroacetic acid in water). The matrix/protein mixture was spotted onto a Bruker Biotarget 48 plate pre-coated with a dried sinapinic acid layer. Mass spectra were acquired using a Bruker microFLEX MALDI-TOF instrument. Theoretical molecular weights were calculated based on the amino acid sequence using the ExPASy Compute pI/Mw tool to confirm purity and identity.

Electrochemical Measurements. All electrochemical measurements were carried out using a CH Instrument 6171B potentiostat. A standard 3-electrode cell was used in all experiments with a basal plane graphite (BPG) working electrode, a platinum counter electrode, and a silver/silver chloride (saturated KCl) reference electrode. Acetate-phosphate-borate (APB) buffer was used for each experiment. The APB buffer composition was: 20 mM sodium acetate, 20 mM sodium phosphate, 20 mM sodium borate, and 100 mM potassium chloride. Potentials were calibrated with respect to cobalt (II)tris(2,2´-bipyridyl) $(PF_6)_2$ at all pH values. Reduction potentials were determined by using DPV over a pH range of 4 to 9. The resulting Pourbaix diagrams were fitted using nonlinear least square algorithm in MATLAB to extract pK_a values for oxidized and reduced states. The function used for fitting has been described in the literature and is set out as follows:

$$E^{\circ\prime}(pH) = E^{\circ\prime}(low\ pH) + \frac{RT}{nF} ln\left(\frac{K_a^{red} + [H^+]}{K_a^{ox} + [H^+]}\right)$$

Where $E^{\circ\prime}$(pH) is the observed formal potential at a given pH $E^{\circ\prime}$(low pH) is the formal potential (pH independent) at acidic pH values, R is the universal gas constant, T is temperature, n is the number of electrons involved in the redox process, F is Faradays' constant, the respective K_a values correspond to the ionization constants of the oxidized and reduced protein states and $[H^+]$ is the proton concentration at a given pH value.

Computational Methods

The coordinates for azurin were taken from the X-ray crystal structure (PDBID 4AZU). That structure has 4 azurin proteins in the unit cell and the "A" chain was selected for simulations. GROMACS 2024.4 was used for subsequent calculations. CHARMM36 forcefield with copper active site parameters from previous work. Missing hydrogens were added programmatically. The protein was solvated in a triclinic box where the edge of the box was at least 1.2 nm from the protein. Water was modeled using the explicit TIP3P model. Ions (Na^+ and Cl^-) were added to produce an overall charge neutral system with ionic strength of 0.1 M. Following solvation and ionic strength adjustment, the system was equilibrated for temperature and pressure. For each protein, 15 ns simulations were carried out. Clusters were identified using the gromos algorithm with a 0.115 nm cutoff and using the last 4 ns of the simulations. RMSD and RMSF plots are given below.

Representative UV-visible spectrum of azurin

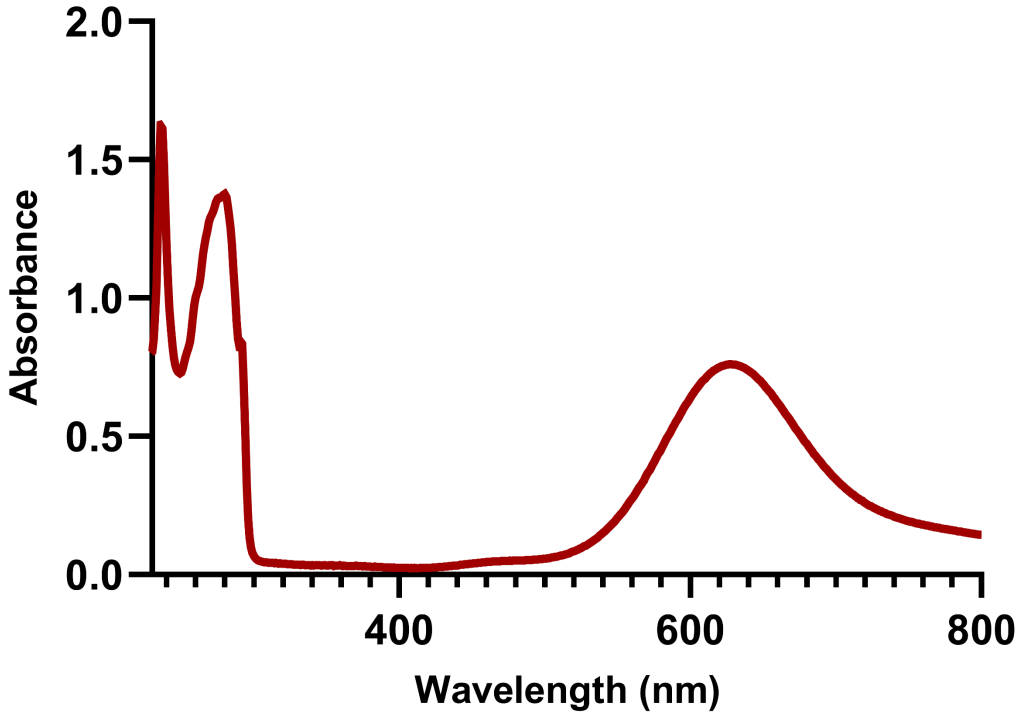

Figure S1. Representative UV-visible spectrum of the azurin variants used in this work. This spectrum is specifically for the H83Q variant (125 μM). Spectra for the other variants are indistinguishable.

MALDI mass spec data for azurin variants

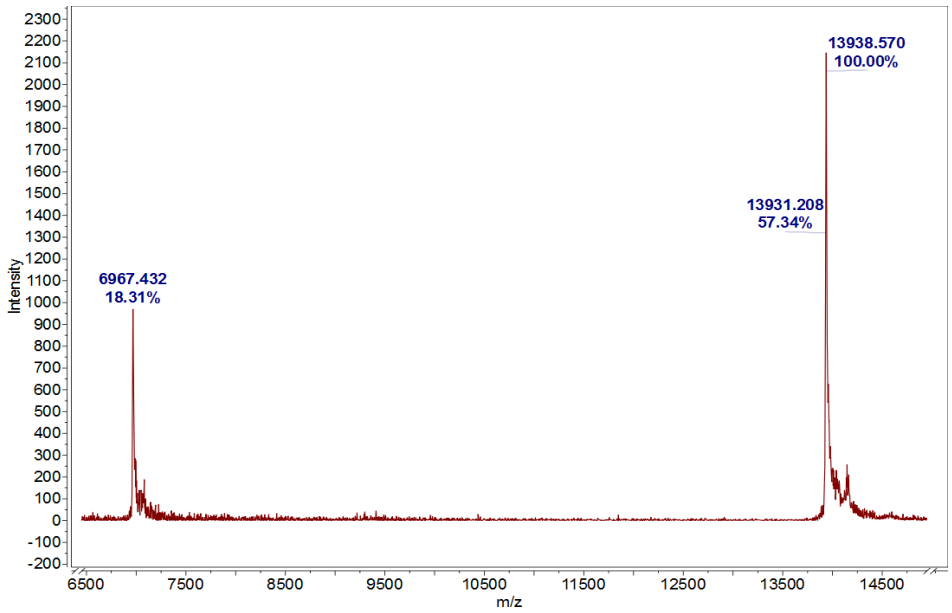

Figure S2. MALDI-TOF mass spec of H83Q azurin (calculated mass: 13937 Da).

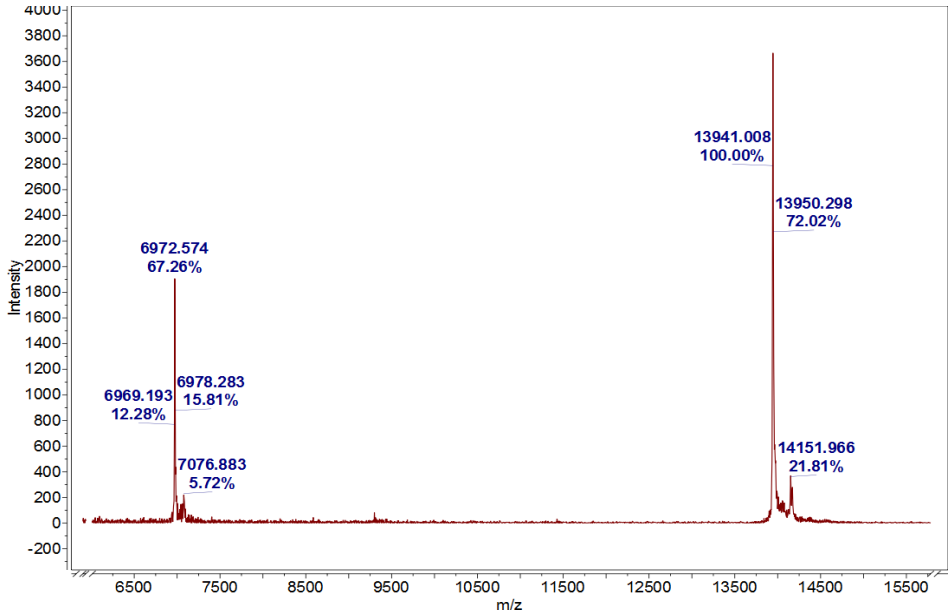

Figure S3. MALDI-TOF mass spectra of H83Q/Q107H azurin (calculated mass: 13946 Da).

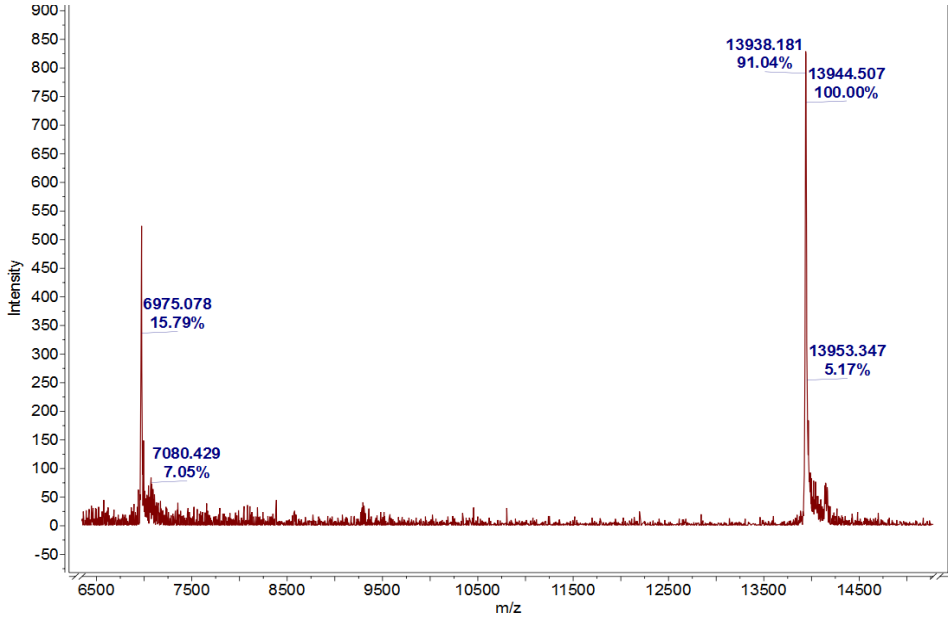

Figure S4. MALDI-TOF mass spectra of H83Q/M109H azurin (calculated mass: 13943 Da).

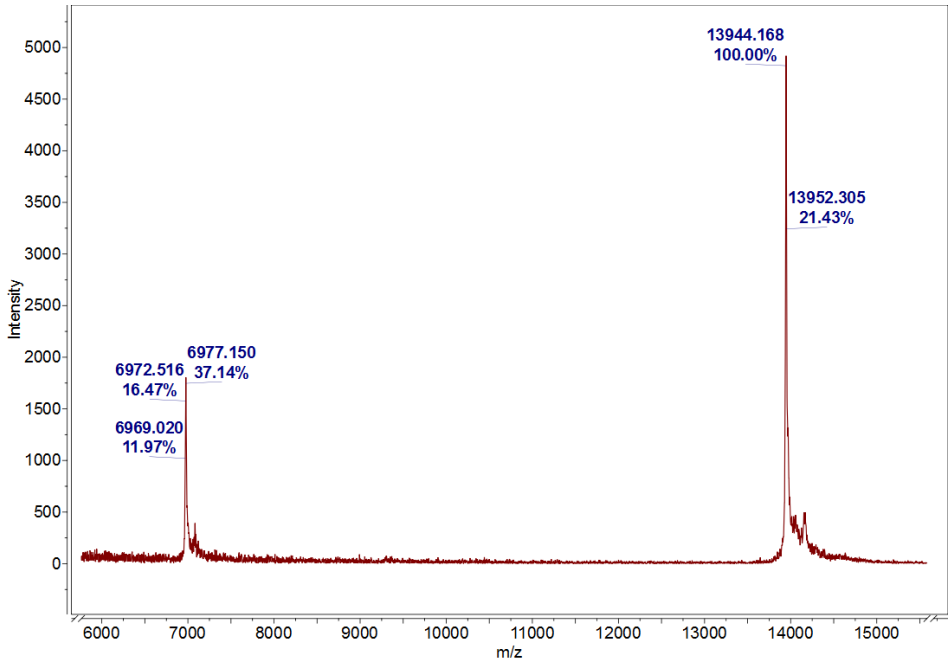

Figure S5. MALDI-TOF mass spectra of H83Q/K122H azurin (calculated mass: 13946 Da).

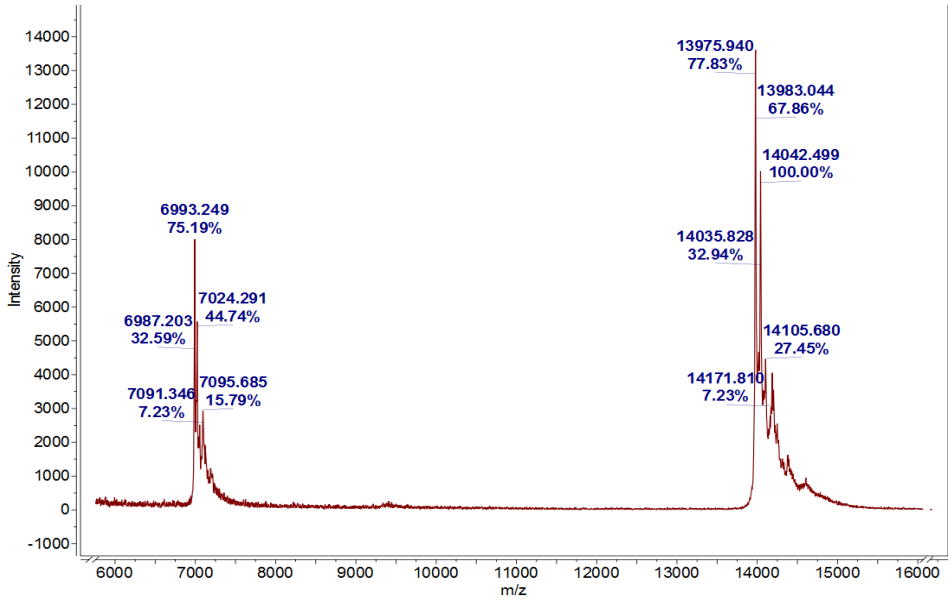

Figure S6. MALDI-TOF mass spec of H83Q/T124H azurin (calculated mass: 13973 Da).

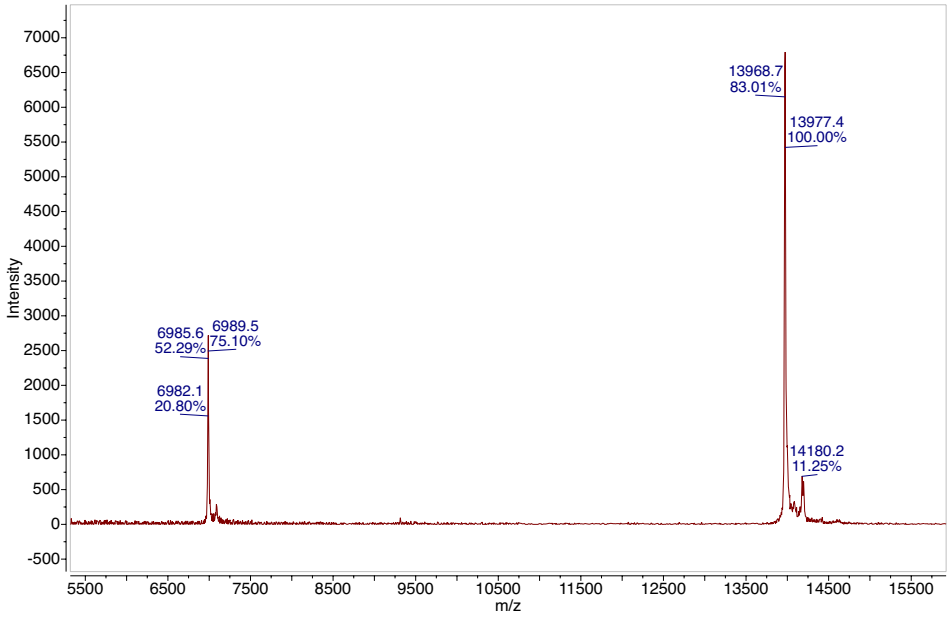

Figure S7. MALDI-TOF mass spec of the H83Q/T126H azurin (calculated mass: 13973 Da).

Example electrochemical data for azurins

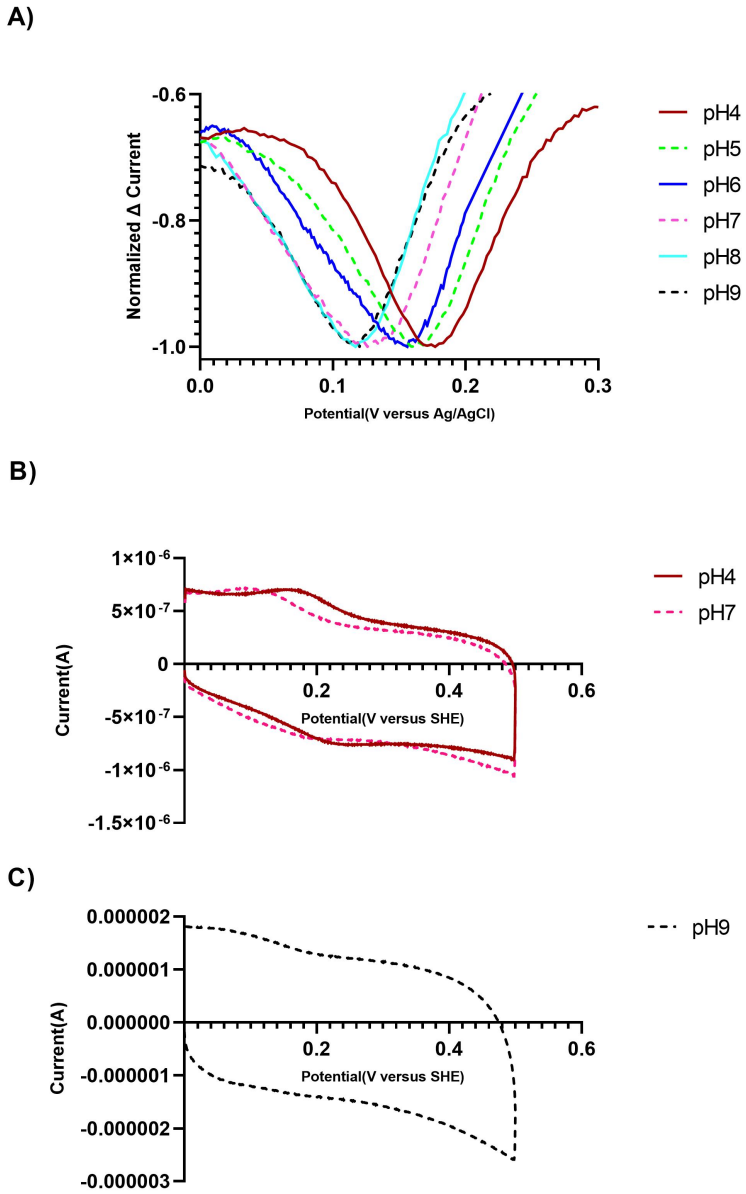

Figure S8. Representative electrochemical data for the azurin variants studied here. These are for H83Q Az at a concentration of 30 μM. The pH values assayed were 4.0 to 9.0. (A) DPV traces showing pH-dependent shifts in midpoint potential. (B) CV traces at pH 4 and pH 7, illustrating the-resolved redox waves at lower pH values. (C) CV trace at pH 9, showing distorted waves due to increased background current. All measurements were performed in 20 mM acetate-phosphate-borate buffers with 100 mM KCl.

Snapshots of histidine local environments in MD cluster structures

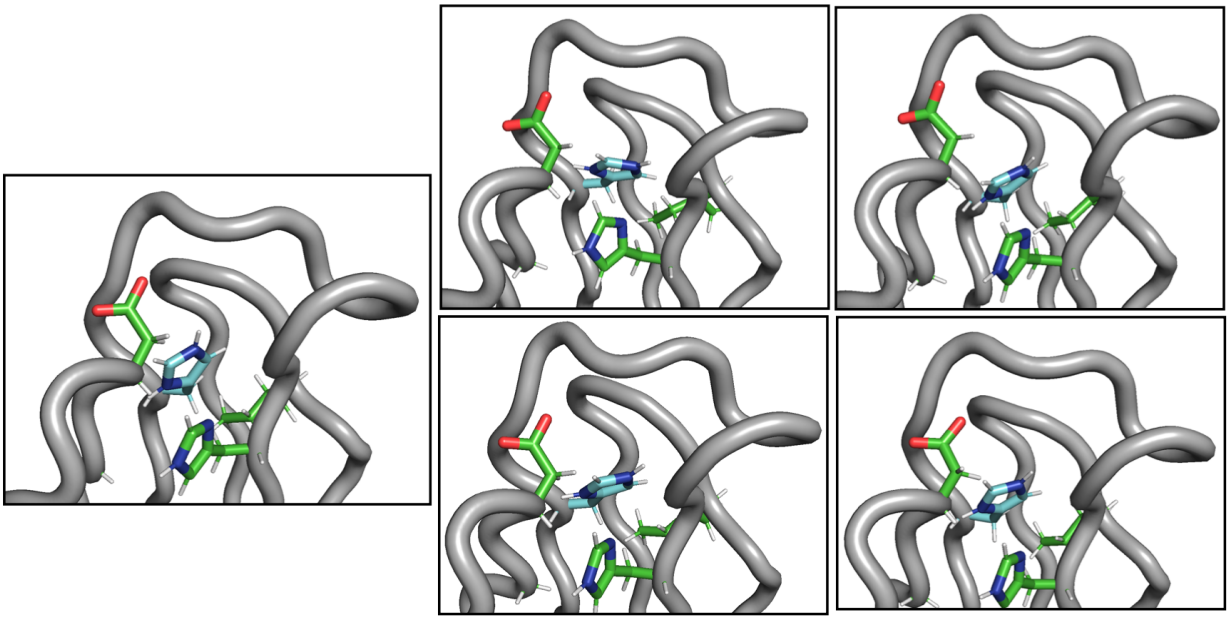

Figure S9. Local environment of H35 in wild type azurin MD cluster structures.

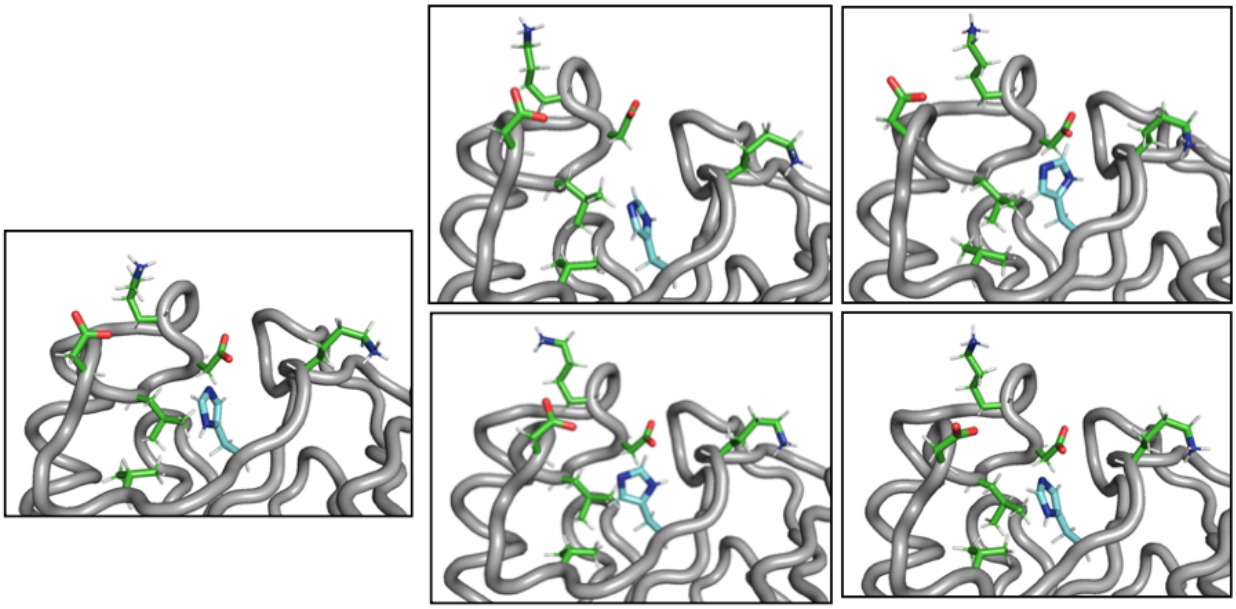

Figure S10. Local environment of H83 in wild type azurin MD cluster structures.

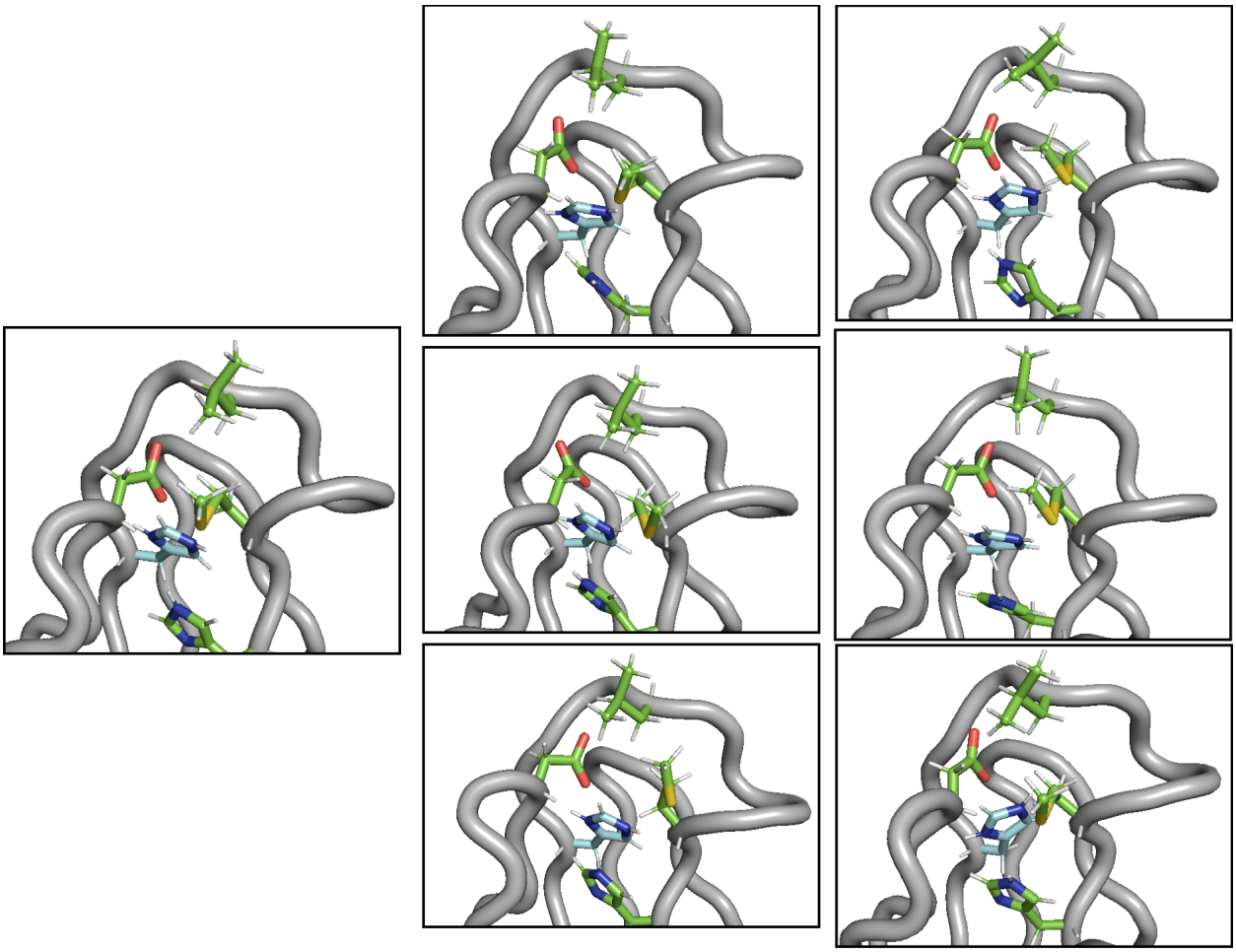

Figure S11. Local environment of H35 in H83Q azurin MD cluster structures.

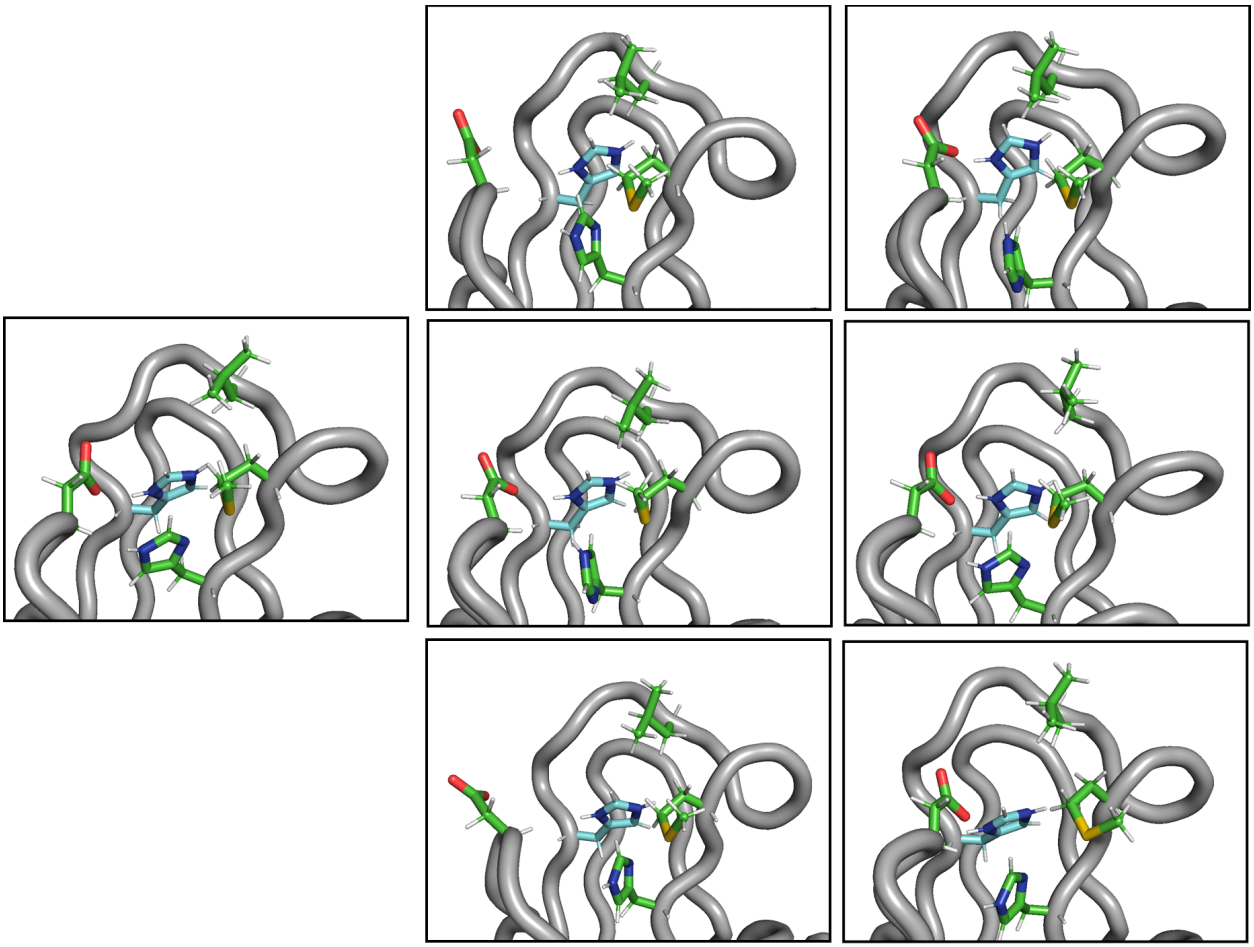

Figure S12. Local environment of H35 in H83Q/Q107H azurin MD cluster structures.

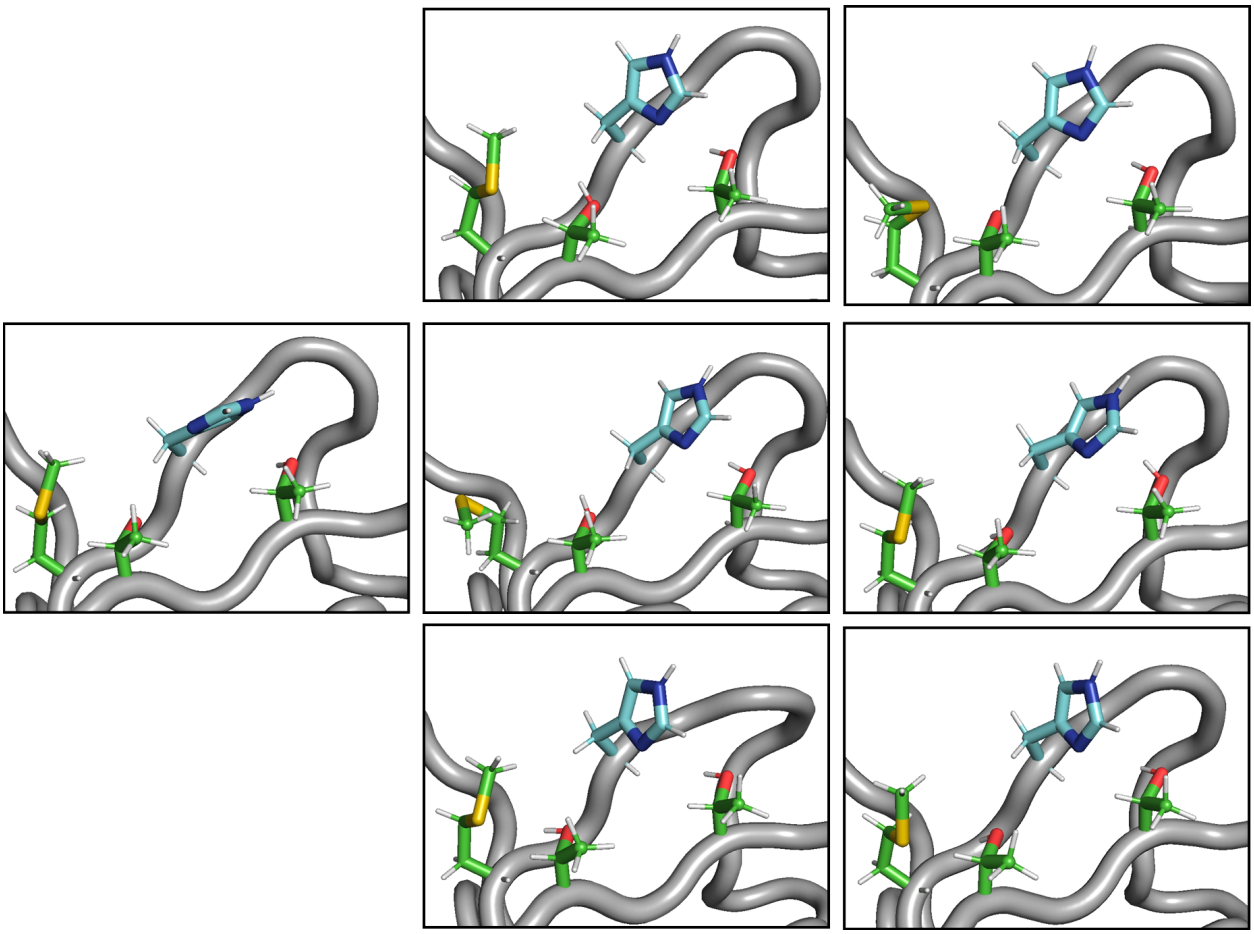

Figure S13. Local environment of H107 in H83Q/Q107H azurin MD cluster structures.

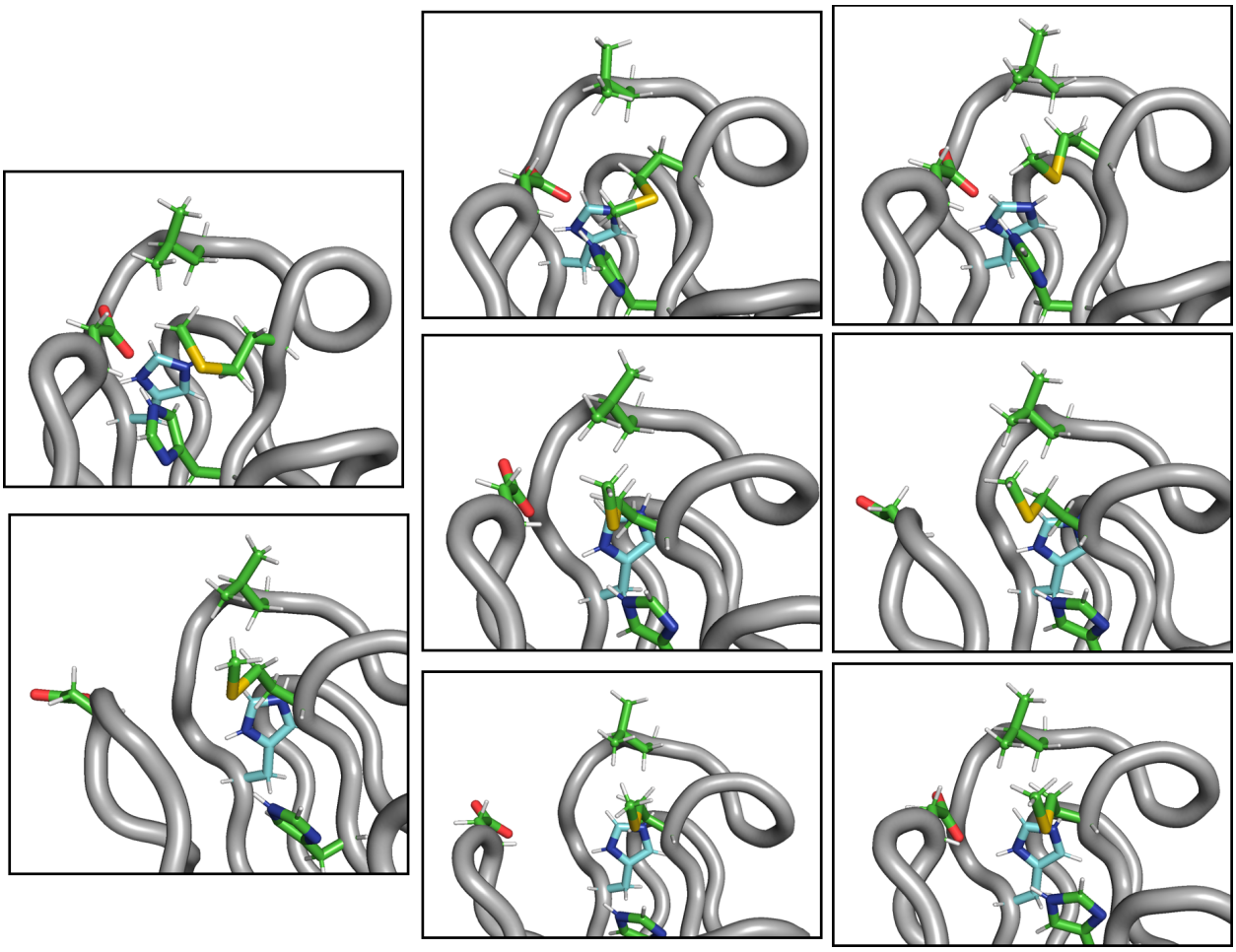

Figure S14. Local environment of H35 in H83Q/M109H azurin MD cluster structures.

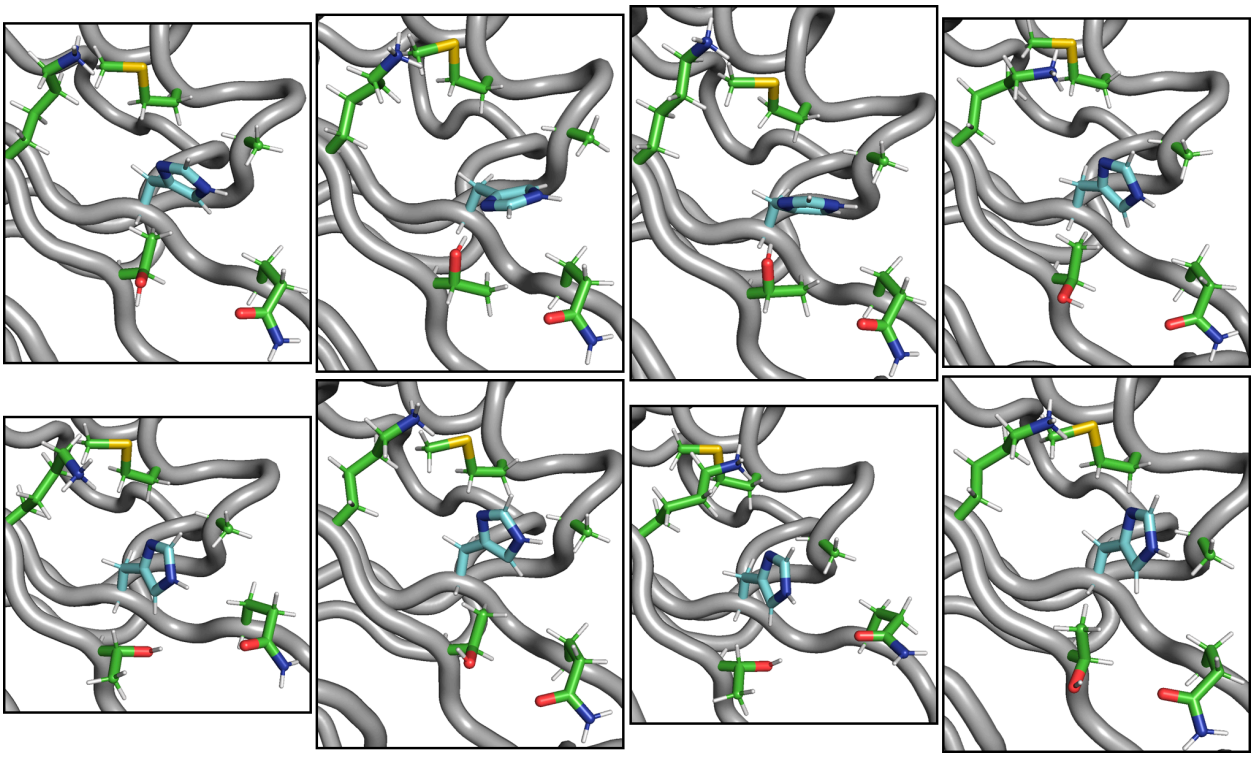

Figure S15. Local environment of H109 in H83Q/M109H azurin MD cluster structures.

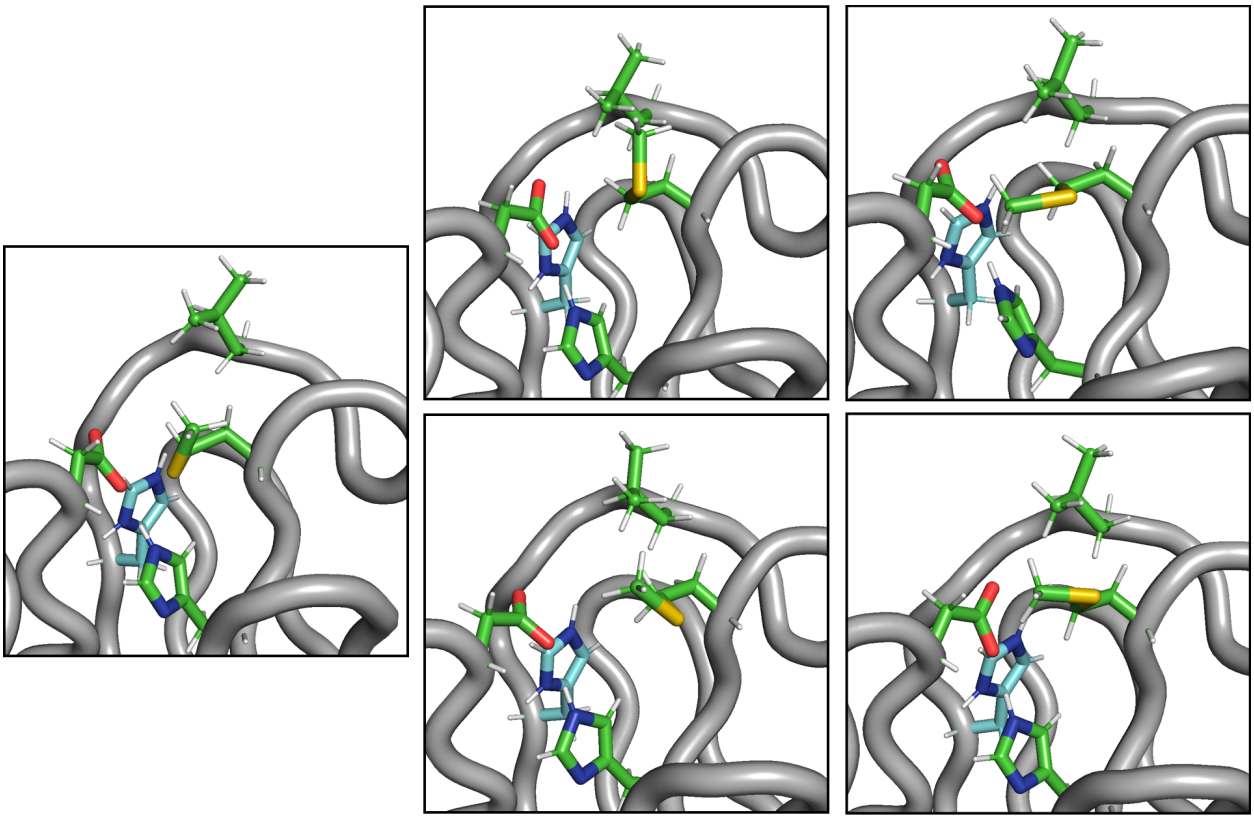

Figure S16. Local environment of H35 in H83Q/K122H azurin MD cluster structures.

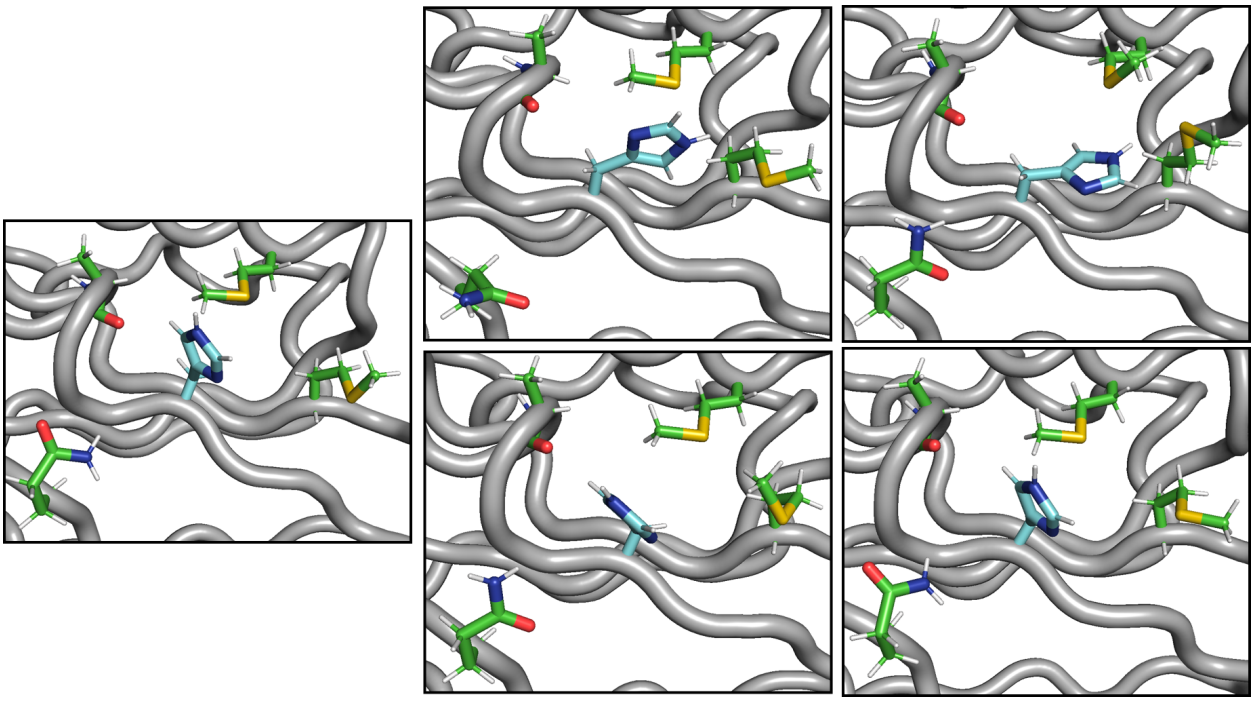

Figure S17. Local environment of H122 in H83Q/K122H azurin MD cluster structures.

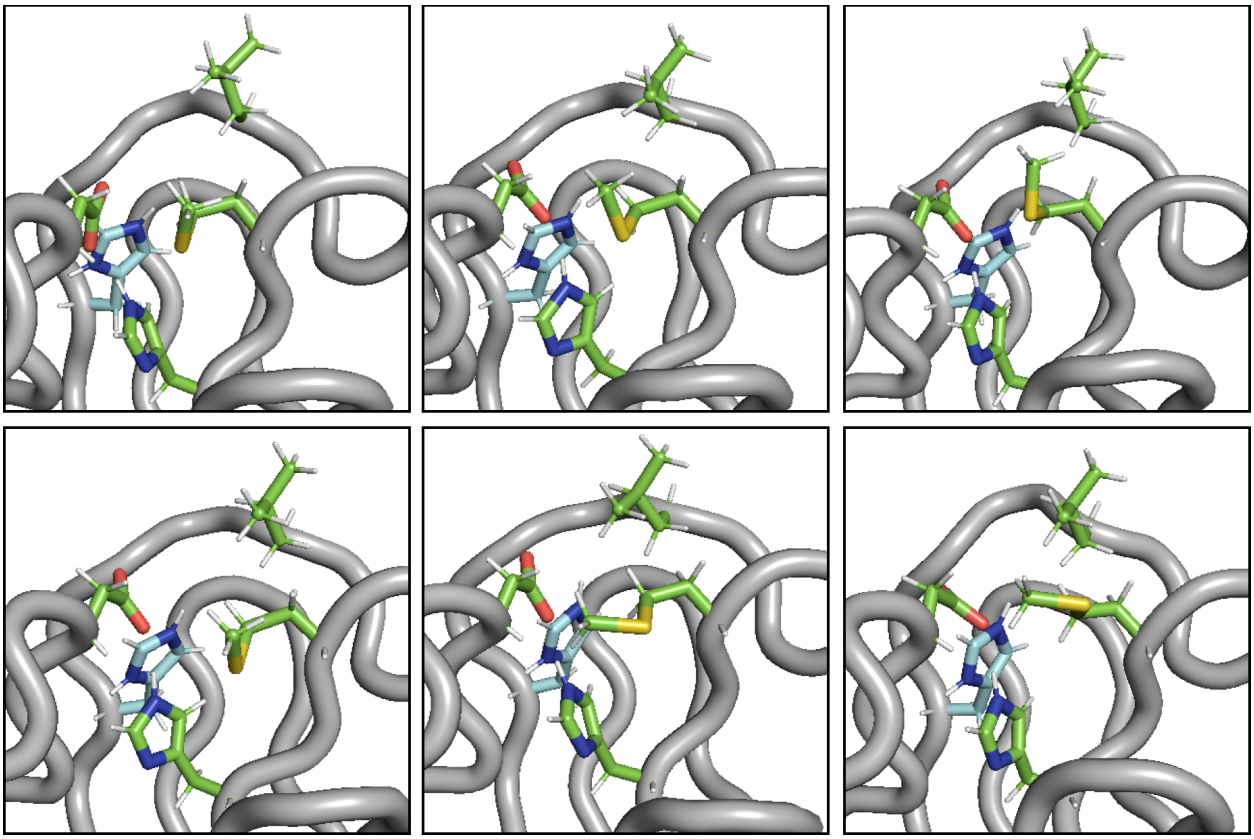

Figure S18. Local environment of H35 in H83Q/T124H azurin MD cluster structures.

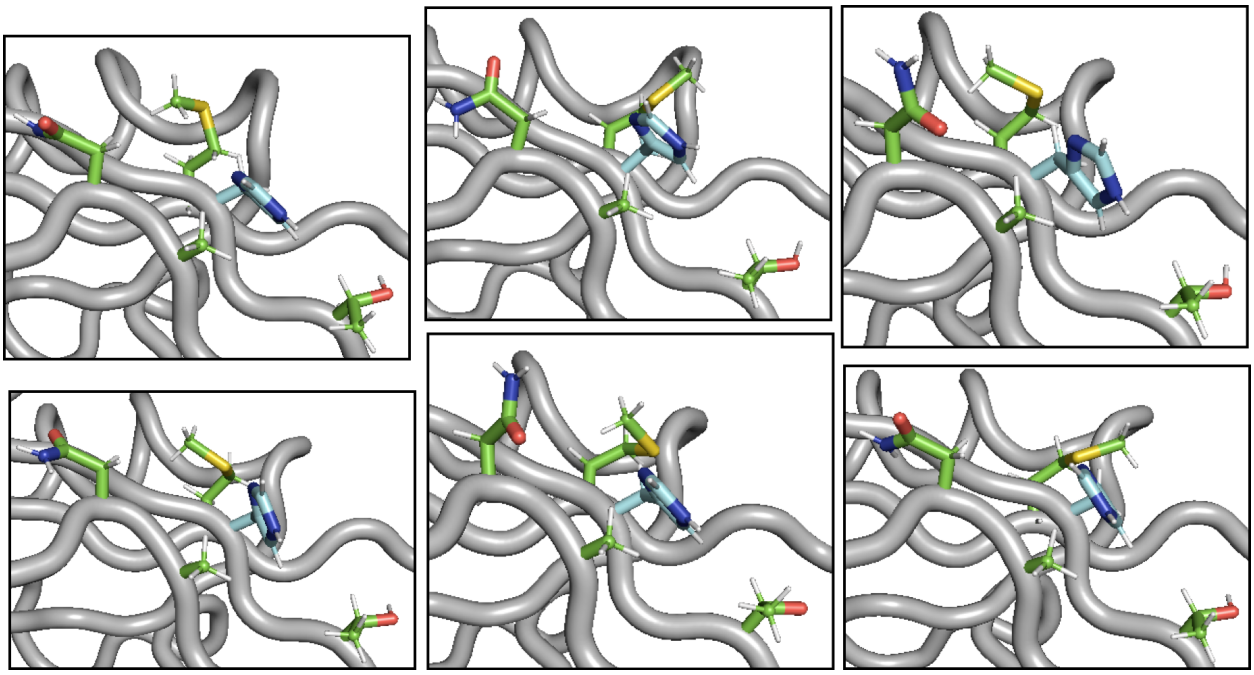

Figure S19. Local environment of H124 in H83Q/T124H azurin MD cluster structures.

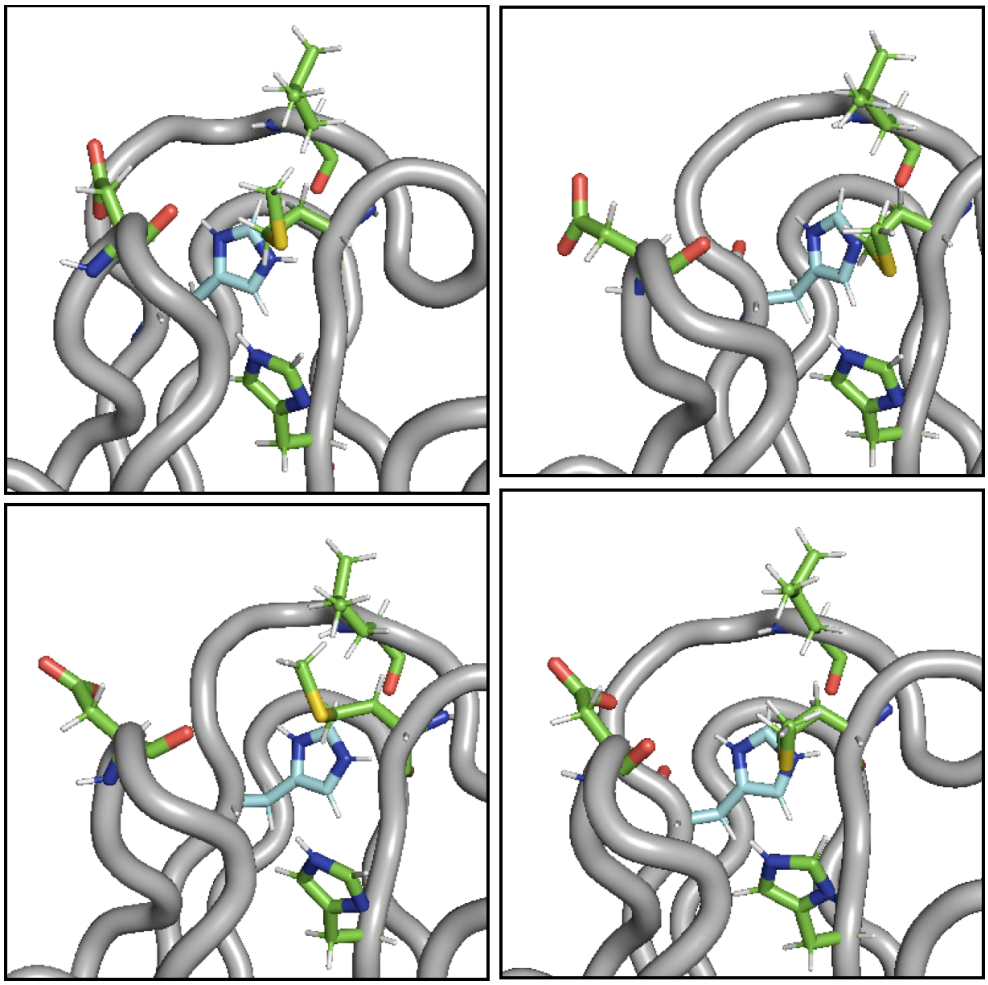

Figure S20. Local environment of H35 in H83Q/T126H azurin MD cluster structures.

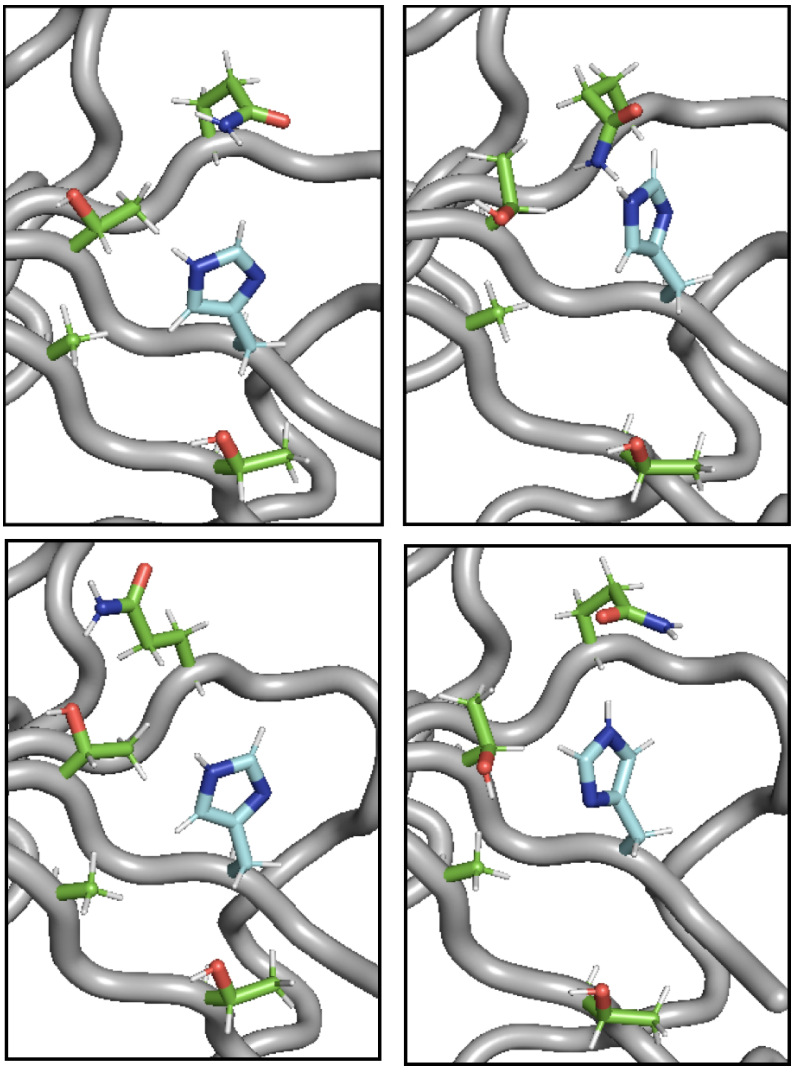

Figure S21. Local environment of H126 in H83Q/T126H azurin MD cluster structures.

Comparison of per-residue fluctuations (RMSF) in MD simulations of azurin.

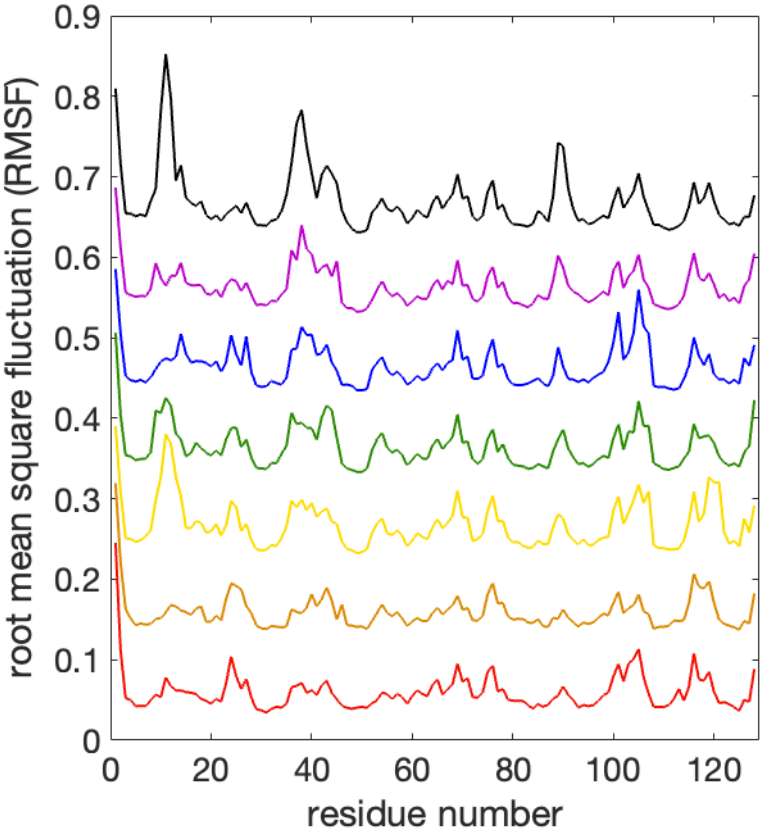

Figure S22. Root mean square fluctuation (RMSF) of the Cα for each amino acid residue in the azurin variants investigated. Each trace is offset vertically by 0.1 nm (1 Å). From bottom to top, the Az variants are: wild type (red), H83Q (orange), H83Q/Q107H (yellow), H83Q/M109H (green), H83Q/K122H (blue), H83Q/T124H (purple), and H83Q/T126H (black).

Comparison of azurin RMSD values over the course of MD simulations.

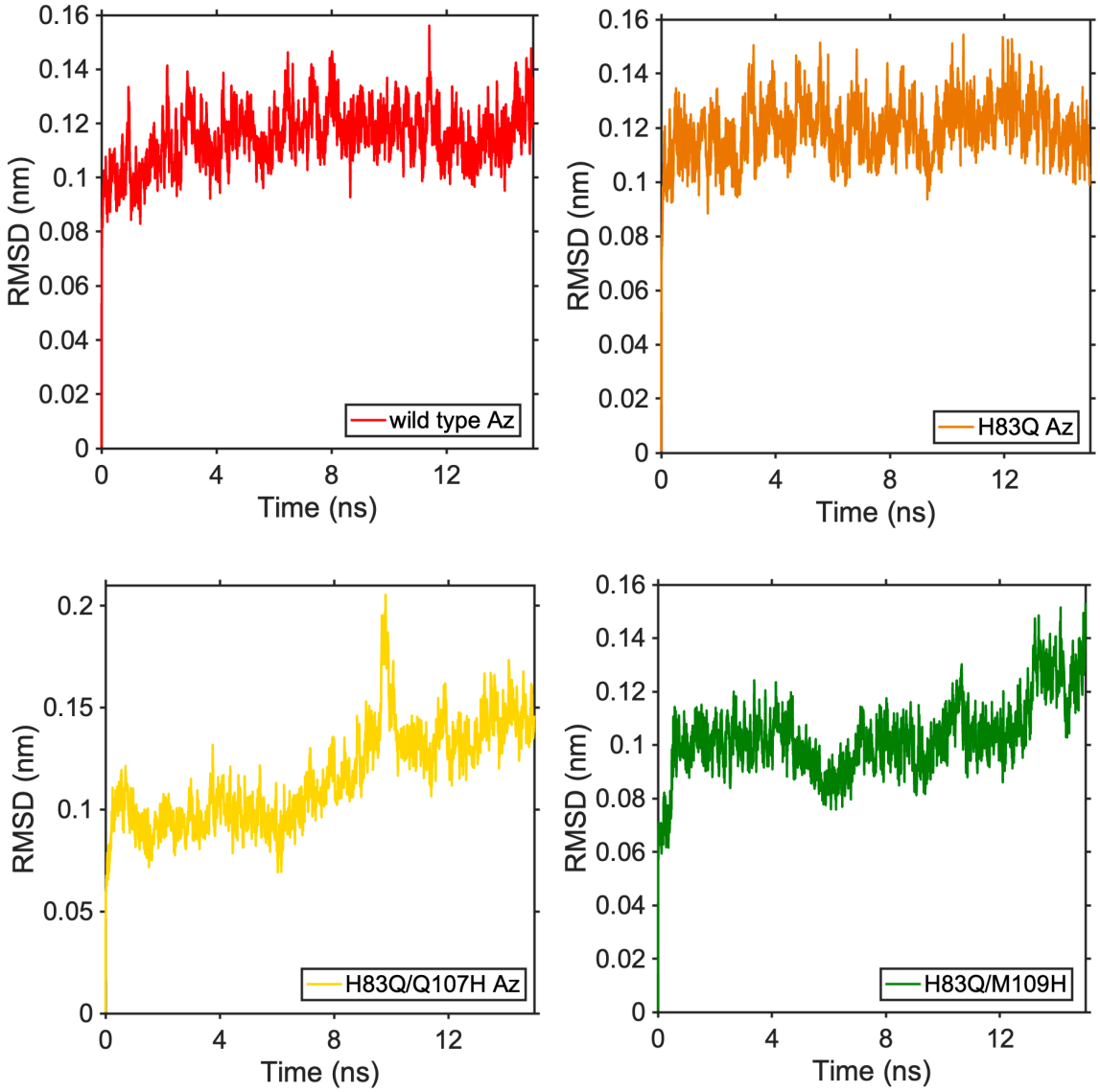

Figure S23 (continues on following page). Root mean square deviation (in nm) of the protein backbone in the azurin variants investigated here. The variants are described in each inset. Wild type (red), H83Q (orange), H83Q/Q107H (yellow), H83Q/M109H (green), H83Q/K122H (blue), H83Q/T124H (purple), and H83Q/T126H (black).

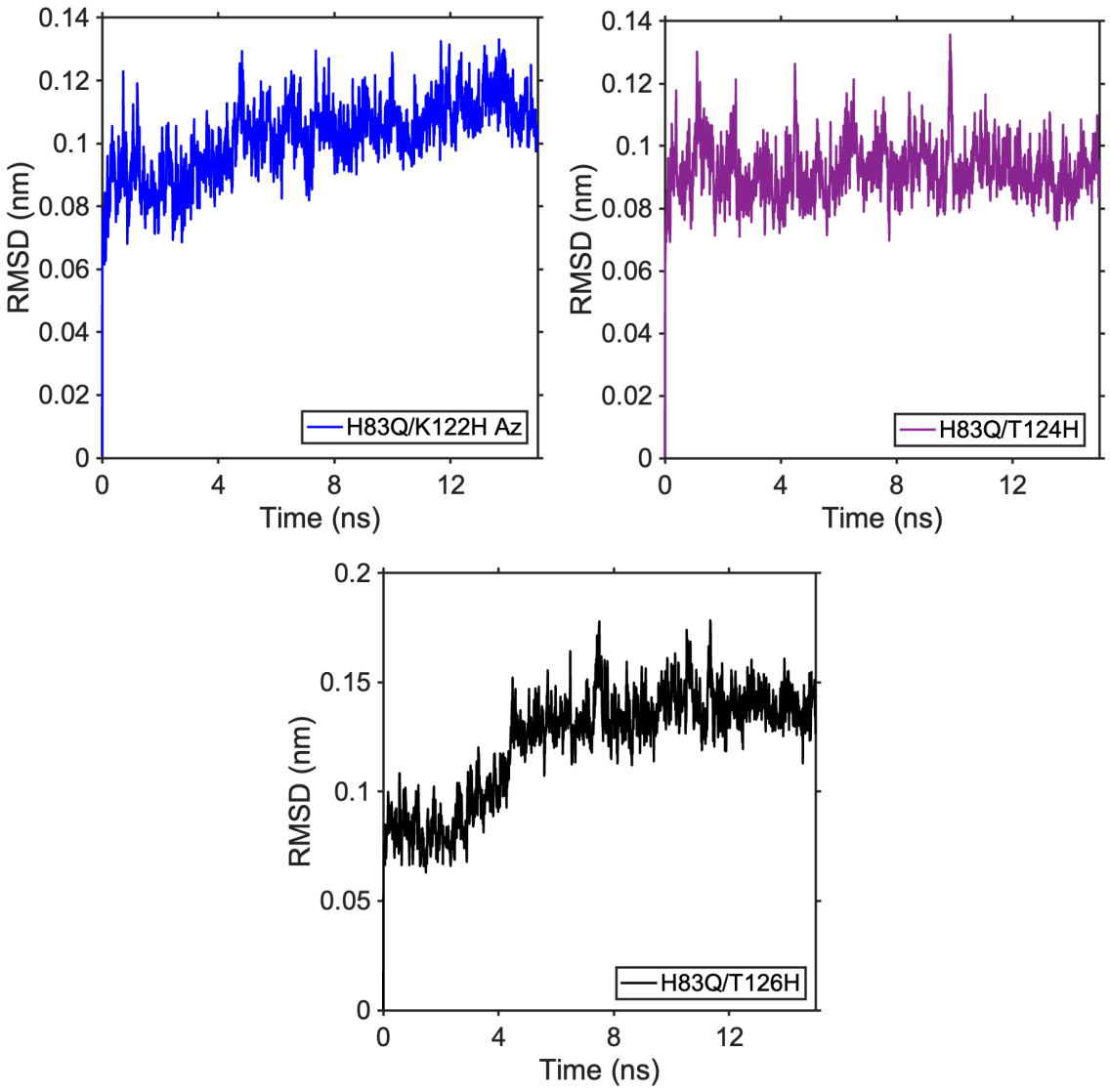

Figure S23 (continues from previous page). Root mean square deviation (in nm) of the protein backbone in the azurin variants investigated here. The variants are described in each inset. Wild type (red), H83Q (orange), H83Q/Q107H (yellow), H83Q/M109H (green), H83Q/K122H (blue), H83Q/T124H (purple), and H83Q/T126H (black).

Computationally predicted histidine pK_a values.

Table S1. Calculated DeepKa values for His in MD-simulated Az structures

Variant	pK_{His35}	pK_{HisX}	pI_{calc}
WT	7.17 ± 0.20	6.96 ± 0.19	4.75
H83Q	7.16 ± 0.37	N/A	4.39
H83Q/Q107H	7.13 ± 0.09	6.76 ± 0.24	4.56
H83Q/M109H	6.98 ± 0.22	6.28 ± 0.11	4.59
H83Q/K122H	7.26 ± 0.23	6.71 ± 0.15	4.49
H83Q/T124H	7.12 ± 0.42	6.52 ± 0.10	4.74
H83Q/T126H	6.88 ± 0.42	6.42 ± 0.22	4.76

[a] Values are given as averages and one standard deviation of all MD clustered structures from gromos analysis

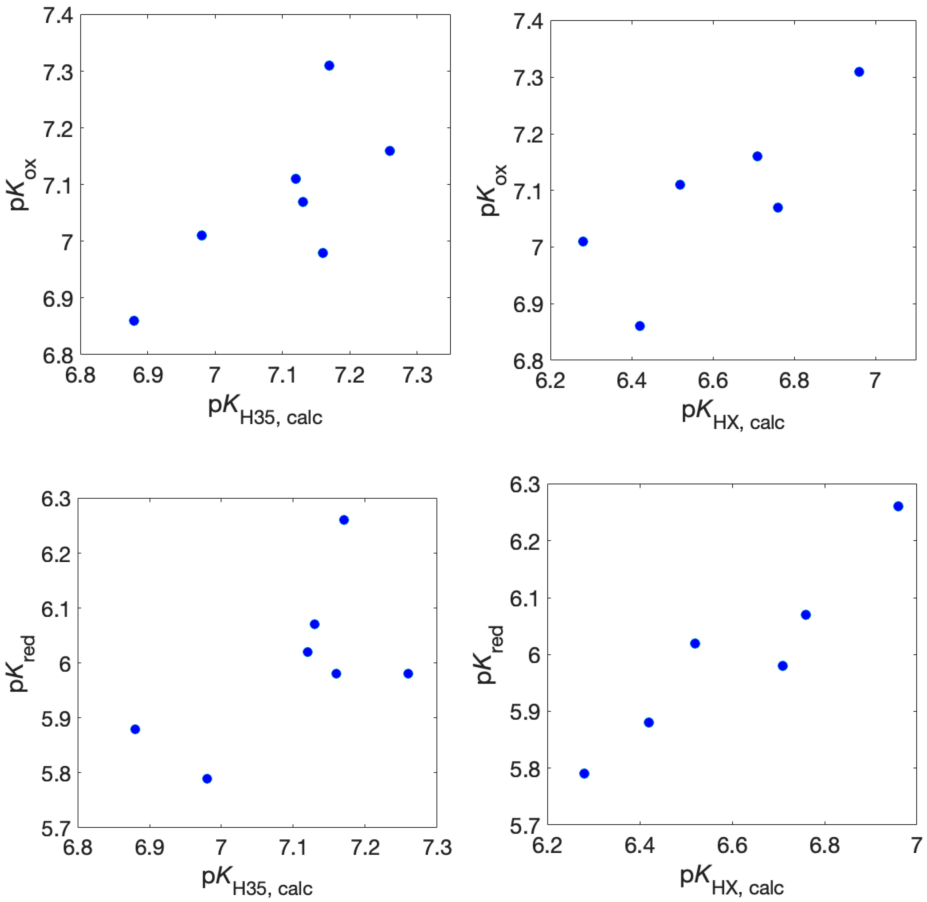

Figure S24. Comparison of individual calculated pK_a values For H35 and HX (X= 83, 107, 109, 122, 124, or 125) and the aggregate pK_{ox} or pK_{red} values from the electrochemical data (i.e., fits to Eqn 1 in the main text).

Plots of p*K* values as a function of Cu-histidine distance

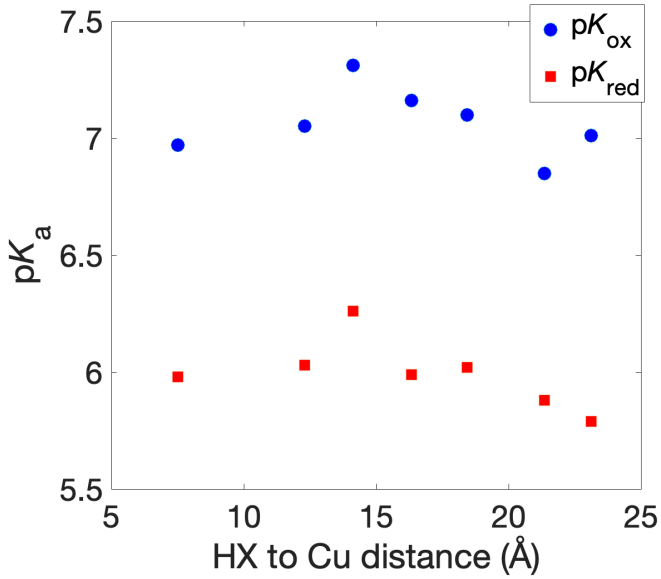

Figure S25. Comparison of pK_{ox} (blue circles) and pK_{red} (red squares) as a function of His-ring to Cu distance. Distances are averages take from the MD-generated cluster structures for each protein. The value at the far left (~7.5 Å) is for H35 in the H83Q Az variant.

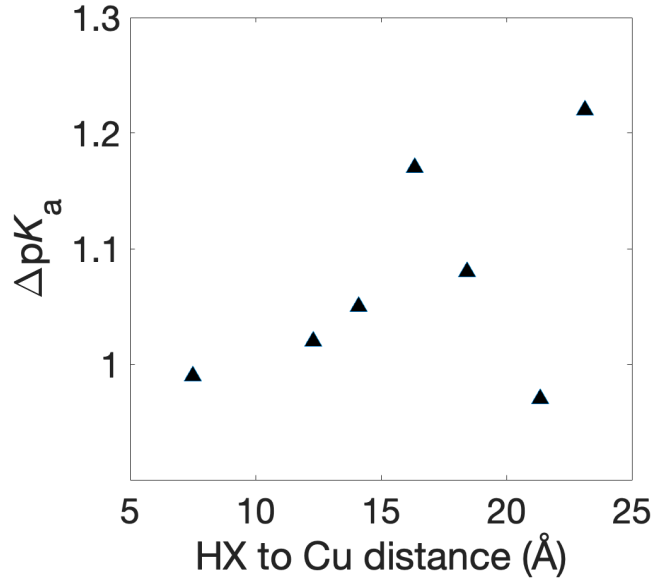

Figure S26. Comparison of Δp*K* (i.e., pK_{ox} – pK_{red}) as a function of His-ring to Cu distance. Distances are averages take from the MD-generated cluster structures for each protein. The value at the far left (~7.5 Å) is for H35 in the H83Q Az variant.

Plots of *E*°′ values as a function of Cu-histidine distance

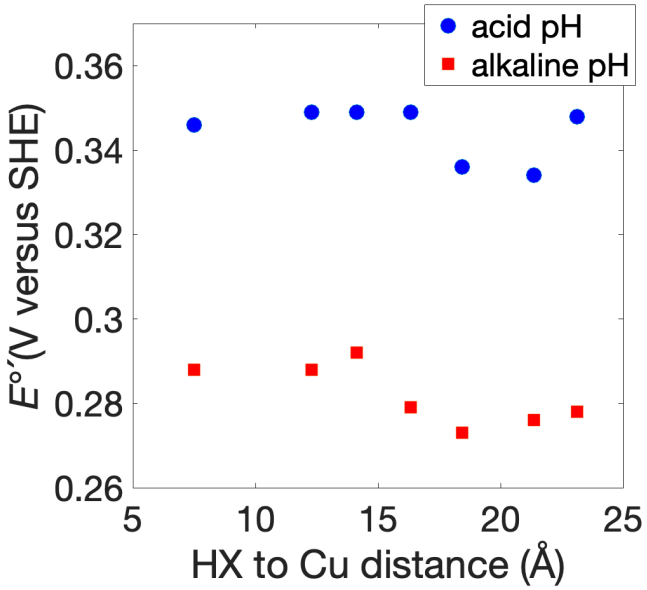

Figure S27. Comparison of *E*°′ values (blue circles for acid pH values and red squares for alkaline pH values) as a function of His-ring to Cu distance. Distances are averages take from the MD-generated cluster structures for each protein. The value at the far left (~7.5 Å) is for H35 in the H83Q Az variant.

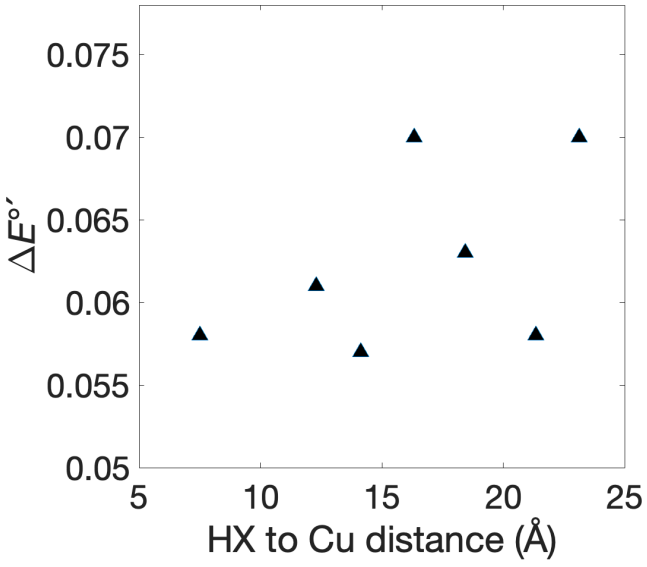

Figure S28. Comparison of Δ*E*°′ (i.e., $E_{high} - E_{low}$) as a function of His-ring to Cu distance. Distances are averages take from the MD-generated cluster structures for each protein. The value at the far left (~7.5 Å) is for H35 in the H83Q Az variant.